

ON MECHANICAL BEHAVIOUR OF PRESSURE-ASSISTED, SINTERED Al-Mg COMPOSITE

Michal Kráčalík

Untere Hauptstraße 48/5, 2424 Zurndorf, Austria, michal.kracalik@gmail.com

Keywords: Al-Mg composite, mechanical behaviour, porosity, finite element simulation

Abstract: Lightweight materials like Al-Mg composite are attractive especially for aerospace or automotive industry. Current paper investigates mechanical behaviour of hot-pressed, reactive sintered Al-Mg composite with initial Mg volume content of 60% using finite element simulation. Conducted numerical simulations study effect of the porosity on mechanical behaviour. Overall porosity (in percent) is decisive factor for mechanical behaviour of investigated Al-Mg composite rather than number or size of pores.

1 Introduction

Lightweight materials like Aluminium (Al)-Magnesium (Mg) composite are in special attraction of automotive and aerospace industry [1-4]. Al-Mg composite combines excellent density of Mg (1.73 g/cm^3) with Al corrosion resistance (density of Al is 2.7 g/cm^3) [2,4].

Particulate reinforced metal matrix composites (MMCs) have isotropic properties, easier processing route than other metal matrix composites and they are cheaper than other metal matrix composites [3]. MMCs (with various reinforcements) can be produced by casting, metal infiltration, friction stir welding or powder metallurgy [3]. Powder metallurgy has an advantage in controlling matrix and reinforcement properties like shape and size of the reinforcement particles, particle distribution and volume fraction in the matrix [3]. However, an inherent characteristic of powder metallurgical components is porosity that influences mechanical behaviour [5-7]. Generally, porosity is characteristic of many engineering materials like concrete [8-11] or soils [12-16].

One promising technology how to deal with porosity in powder metallurgy is the usage of pressure-assisted reactive sintering [17] - practically porous free samples with relative high density were produced for instance in [18,19].

Pressure-assisted reactive sintering was used to produce many (also non-metal) composites such as $\text{ZrB}_2\text{-SiC-ZrC}$ [20], $\text{B}_4\text{C/Li}_2\text{O-Al}_2\text{O}_3\text{-SiO}_2$ [21], Al-Si [22], $\text{ZrB}_2\text{-SiC-ZrO}_2$ [23], $\text{TiC/Ti}_3\text{SiC}_2$ [24] or reinforced Al matrix composites [3] [25]. Depending on material and processing conditions, porosity varied between 2.4% [21] and 26% [24]. Al-NiO composite had a porosity between 5-8.7% [25] and no porosity measurement was conducted for Al-Mg composite in [3]. Contrary to discussed effect of the porosity on the mechanical behaviour in additive manufacturing (AM) [26-27], it seems to be relatively lack of the information about the quantitative effect of the porosity on the mechanical behaviour of the Al-Mg composite produced by pressure-assisted reactive sintering. Therefore, the aim of the paper is studying effect of the porosity on the mechanical behaviour of Al-Mg

composite. Mechanical behaviour of Al-Mg composite with initial Mg volume content of 60% is investigated using FE simulation.

2 Finite element and material model

2D finite element (FE) model consists of one square shaped part with size of $100 \times 100 \mu\text{m}$ with plane strain thickness of $100 \mu\text{m}$. Pores are embedded in the model as free space in the solid volume. Pores positions are created with Python numpy library with uniform distribution over the size of the FE model ($100 \times 100 \mu\text{m}$) and imported to FE software Ansys. The size of the pores is chosen to produce 1% and 2% porosity in the FE model. 10 and 20 pores are created in the FE model with diameter d approximately $3.57 \mu\text{m}$, respectively $5.05 \mu\text{m}$. FE model is fixed at the bottom edge and loaded on the top edge with tensile loading 400 MPa . Mesh element size is $1 \mu\text{m}$ in the whole FE model. Scheme and size of the FE is shown in Figure 1.

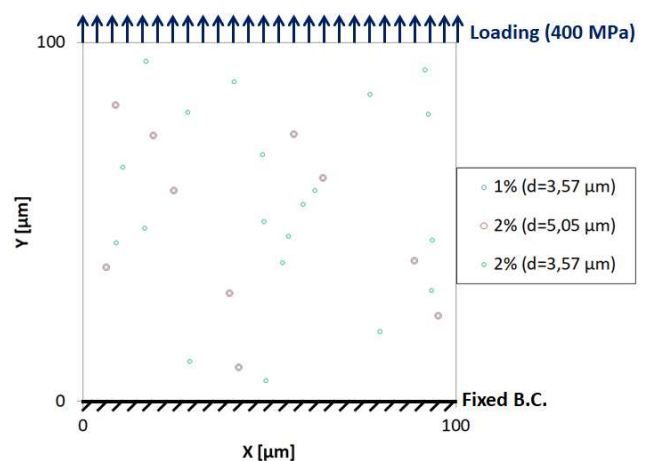


Figure 1 Scheme and size of the FE model. Legend describes the size of the pores in the FE model. 1% and 2% porosity is created in the FE model by varying the pore diameter d and number of pores. FE Model is loaded on the top edge with tensile load 400 MPa

Material model is based on the measurement presented in [3]. There were Al and Mg powders blended by

ON MECHANICAL BEHAVIOUR OF PRESSURE-ASSISTED, SINTERED Al-Mg COMPOSITE
 Michal Kráčalík

planetary ball mill at rotational speed 100 RPM under argon atmosphere for 1 hour, hot-pressed at temperature 673 K under pressure 640 MPa for 10 minutes under Argon atmosphere and reinforced with Al_3Mg_2 and $Al_{12}Mg_{17}$ intermetallics produced during the pressure-assisted sintering process. Details about the production process and produced microstructure are described in the referenced paper [3].

Figure 2 shows material model of Al-Mg hot-pressed, reactive sintered composite with initial Mg volume content $V=60\%$ taken from [3] (Denotes as “Shahid2018” in the legend).

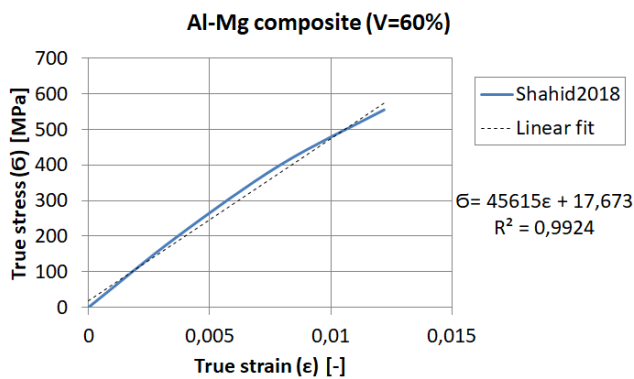


Figure 2 Al-Mg hot-pressed, reactive sintered composite with Mg volume content $V=60\%$. Measured data is taken from [3]. Measured data is linearly fitted with a resulting coefficient of determination R^2 greater than 0.99

Measured data is linearly fitted with a resulting coefficient of determination R^2 greater than 0.99. Value 45615 represents according to Hooke’s law Young’s modulus E . Hence, the material behaviour is (almost) linear elastic, the linear-elastic material model is used in the FE simulation. The yield strength σ_y and tensile strength σ_{TS} are both set on 574 MPa (see Figure 2).

3 Results

Stress behaviour is for comparison expressed by safety factor simply as $F = \sigma_1 / \sigma_{TS}$ (Maximum tensile stress failure theory), where σ_1 is maximal principal stress. It can be shown that σ_1 corresponds with σ_Y (stress component in the loading direction, see Figure 1). Maximal principal stress criterion has been identified as suitable for describing failure in presence of defects (pores) in brittle materials [26,28].

Presented Safety factor can be viewed only as a comparison measure among presented model variations.

Figure 3 shows Safety factor F distribution for 1% porosity FE model with pore diameter $d=3.57 \mu m$. Distribution of the safety factor around all pores show similar behaviour – Minimum safety factor F is calculated perpendicular to the loading direction. Pores are stretched in the deformation direction (Y-Axis). It can be assumed that crack would start to initiate and growth in Mode I from

the marked position with minimum safety factor where maximum principal stresses occur.

According to given safety factor definition: $F=0.44572$ gives maximal principal stress σ_1 approximately equal to 1288 MPa. Safety factor outside pores lies approximately between 1.2÷1.4 in almost whole FE model.

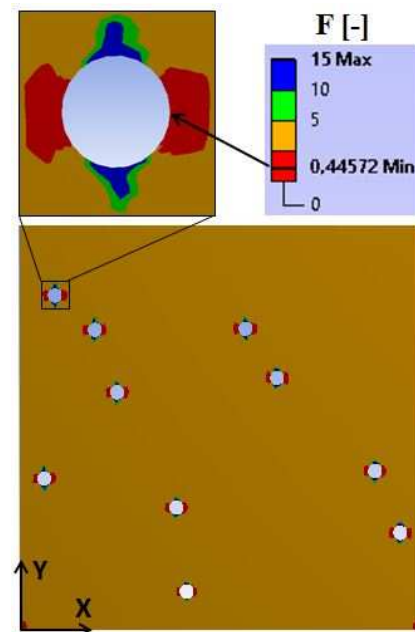


Figure 3 Safety factor F distributions in FE model with detailed view on the most critical position. Minimum calculated safety factor $F=0.44572$ corresponds with maximum principal stresses approximately of 1288 MPa. Safety factor (stress) distribution is similar around all pores in the FE model

Figure 4 shows summarisation of the results. Minimum safety factor F is in free porous FE model (0% porosity) approximately 1.4. It corresponds roughly with maximum principal stresses σ_1 of 400 MPa. 400 MPa is given loading in the FE model - the FE model is verified.

Figure 4 shows a minimal safety factor for 0% (porous free FE model), 1% and 2% porosity. Free porous FE model gives the highest safety factor almost 1.4 and the smallest safety factor 0.365 is calculated for 2% porosity with 20 pores ($d=3.57 \mu m$). Pores reduce safety factor significantly going from free porous FE model to 1% porosity. Porosity is changed negligible between 1% and 2% porosity. Values are taken from whole model and a minimum value is not located in the one position.

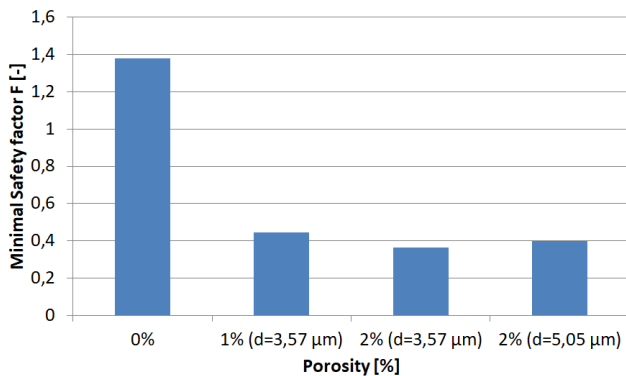
ON MECHANICAL BEHAVIOUR OF PRESSURE-ASSISTED, SINTERED Al-Mg COMPOSITE
 Michal Kráčalík


Figure 4 Minimal Safety factor F for 0% (free porous FE model), 1% and 2% porosity. 2% porosity with 20 pores $d=3,57 \mu\text{m}$ gives the smallest safety factor. The highest safety factor is calculated for free porous FE model

Figure 5 shows Maximal displacement U_y in the Y direction (see Figure 3) for free porous FE model, 1% and 2% porosity. Highest displacement is calculated for 2% porosity with 10 pores ($d=5.05 \mu\text{m}$). Smallest displacement is calculated for free porous FE model.

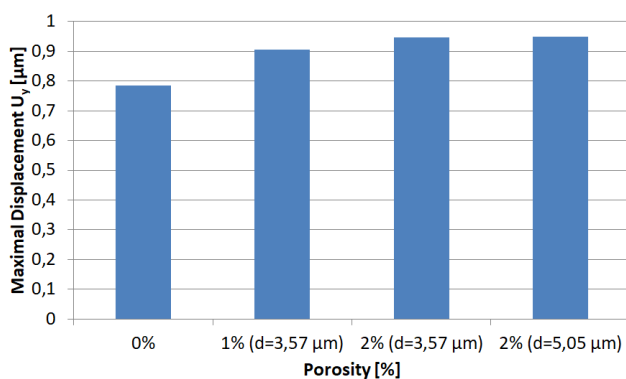


Figure 5 Maximal displacement U_y for 0% (free porous FE model), 1% and 2% porosity. 2% porosity with 10 pores $d=5.05 \mu\text{m}$ gives highest displacement. Smallest displacement is calculated for free porous FE model

Figure 4 and 5 show significant different between free porous FE model and porous FE models. Stress behaviour (expressed through Safety factor F in Figure 4) demonstrates bigger differences than displacement (Figure 5) among free porous FE model and porous FE models. Differences between 1% and 2% porosity are less pronounced and no conclusion can be made about number and size of pores (2% porosity). Only the overall porosity (in %) regardless size and number of pores is decisive for the mechanical behaviour of Al-Mg composite with initial Mg volume content $V=60\%$.

Conclusions

This paper investigates effect of porosity on the mechanical behaviour of hot-pressed, reactive sintered Al-Mg composite. Al-Mg composite with initial Mg volume content of 60% has been investigated by means of finite

element simulation. Simulations show that overall porosity (in %) has a more pronounced effect on the mechanical behaviour than number or size of pores. The effect is more prominent for stress behaviour (expressed through Safety factor F) than for displacement.

References

- [1] KITTNER, K., FEUERHACK, A., FÖRSTER, W., BINOTSCH, C., GRAF, M.: *Recent Developments for the Production of Al-Mg Compounds*, Materials Today, Proceedings, Vol. 2, pp. S225 - S232, 2015.
- [2] PARK, K., PARK, J., KWON, H.: Effect of intermetallic compound on the Al-Mg composite materials fabricated by mechanical ball milling and spark plasma sintering, *Journal of Alloys and Compounds*, Vol. 739, pp. 311-318, 2018.
- [3] SHAHID, R.N., SCUDINO, S.: Microstructure and Mechanical Behavior of Al-Mg Composites Synthesized by Reactive Sintering, *Metals*, Vol. 8, 2018.
- [4] GAO, T., LI, Z., HU, K., HAN, M., LIU, X.: Synthesizing (ZrAl₃ + AlN)/Mg–Al composites by a ‘matrix exchange’ method, *Results in Physics*, Vol. 9, pp. 166-170, 2018.
- [5] DUNSTAN, M.K., PARAMORE, J.D., FANG, Z.Z.: The effects of microstructure and porosity on the competing fatigue failure mechanisms in powder metallurgy Ti-6Al-4V, *International Journal of Fatigue*, Vol. 116, pp. 584-591, 2018.
- [6] LI, X., OLOFSSON, U.: A study on friction and wear reduction due to porosity in powder metallurgic gear materials, *Tribology International*, Vol. 110, pp. 86-95, 2017.
- [7] PARK, J., LEE, S., KANG, S., JEON, J., LEE, S.H., KIM, H.-K., CHOI, H.: Complex effects of alloy composition and porosity on the phase transformations and mechanical properties of powder metallurgy steels, *Powder Technology*, Vol. 284, pp. 459-466, 2015.
- [8] LI, D., LI, Z., LV, C., ZHANG, G., YIN, Y.: A predictive model of the effective tensile and compressive strengths of concrete considering porosity and pore size, *Construction and Building Materials*, Vol. 170, pp. 520-526, 2018.
- [9] LIAN, C., ZHUGE, Y., BEECHAM, S.: The relationship between porosity and strength for porous concrete, *Construction and Building Materials*, Vol. 25, pp. 4294-4298, 2011.
- [10] ZINGG, L., BRIFFAUT, M., BAROTH, J., MALECOT, Y.: Influence of cement matrix porosity on the triaxial behaviour of concrete, *Cement and Concrete Research*, Vol. 80, pp. 52-59, 2016.

ON MECHANICAL BEHAVIOUR OF PRESSURE-ASSISTED, SINTERED Al-Mg COMPOSITE

Michal Kráčalík

- [11] BENOUIS, A., GRINI, A.: Estimation of Concrete's Porosity by Ultrasounds, *Physics Procedia*, Vol. 21, pp. 53-58, 2011.
- [12] CHOO, H., JUN, H., YOON, H.-K.: Porosity estimation of unsaturated soil using Brutsaert equation, *Soil Dynamics and Earthquake Engineering*, Vol. 104, pp. 33-39, 2018.
- [13] HOLTHUSEN, D., BRANDT, A.A., REICHERT, J.M., HORN, R.: Soil porosity, permeability and static and dynamic strength parameters under native forest/grassland compared to no-tillage cropping, *Soil and Tillage Research*, Vol. 177, pp. 113-124, 2018.
- [14] MUNKHOLM, L.J., HECK, R.J., DEEN, B., ZIDAR, T.: Relationship between soil aggregate strength, shape and porosity for soils under different long-term management, *Geoderma*, Vol. 268, pp. 52-59, 2016.
- [15] TSENG, C.L., ALVES, M.C., MILORI, D. M. B. P., CRESTANA, S.: Geometric characterization of soil structure through unconventional analytical tools, *Soil and Tillage Research*, Vol. 181, pp. 37-45, 2018.
- [16] PIRES, L.F., BRINATTI, A.M., SAAB, S.C., CÁSSARO, F.A.M.: Porosity distribution by computed tomography and its importance to characterize soil clod samples, *Applied Radiation and Isotopes*, Vol. 92, pp. 37-45, 2014.
- [17] NOVÁK, P., MICHALCOVÁ, A., VODĚROVÁ, M., ŠÍMA, M., ŠERÁK, J., VOJTĚCH, D., WIENEROVÁ, K.: Effect of reactive sintering conditions on microstructure of Fe-Al-Si alloys, *Journal of Alloys and Compounds*, Vol. 493, pp. 81-86, 2010.
- [18] TOSCANO, J.A.G., FLORES, A.V., SALINAS, A.R., NAVA, E.V.: Microstructure of Al₉(MnFe)_xSi intermetallics produced by pressure-assisted reactive sintering of elemental AlMnFeSi powder mixtures, *Materials Letters*, Vol. 57, pp. 2246-2252, 2003.
- [19] GAN, L., PARK, Y.-J., ZHU, L.-L., GO, S.-I., KIM, H., KIM, J.-M., KO, J.-W.: Fabrication of transparent LaYZr₂O₇ ceramic by reactive hot-pressing sintering from commercial raw powders, *Materials Letters*, Vol. 189, pp. 256-258, 2017.
- [20] QIANG, Q., XINGHONG, Z., SONGHE, M., WENBO, H., CHANGQING, H., JIECAI, H.: Reactive hot pressing and sintering characterization of ZrB₂-SiC-ZrC composites, *Materials Science and Engineering: A*, Vol. 491, pp. 117-123, 2008.
- [21] XIA, L., ZHONG, B., SONG, T., WU, S., ZHANG, T., WEN, G.: Reactive hot pressing and mechanical properties of B₄C/Li₂O-Al₂O₃-SiO₂ composites, *Journal of Non-Crystalline Solids*, Vol. 432, pp. 510-518, 2016.
- [22] EJIORFOR, J.U., REDDY, R.G.: Characterization of pressure-assisted sintered Al-Si composites, *Materials Science and Engineering: A*, Vol. 259, pp. 314-323, 1999.
- [23] VAFA, N.P., ASL, M.S., ZAMHARIR, M.J., KAKROUDI, M.G.: Reactive hot pressing of ZrB₂-based composites with changes in ZrO₂/SiC ratio and sintering conditions. Part I: Densification behavior, *Ceramics International*, Vol. 41, pp. 8388-8396, 2015.
- [24] LO, W.-T., NAYAK, P.K., LU, H.-H., LII, D.-F., HUANG, J.-L.: Evolution of binary phase TiC/Ti₃SiC₂ composites from TiC/Ti/Si by hot-pressed reactive sintering, *Materials Science and Engineering: B*, Vol. 172, pp. 18-23, 2010.
- [25] FOGAGNOLO, J.B., PALLONE, E.M.J.A., MARTIN, D.R., KIMINAMI, C.S., BOLFARINI, C., BOTTA, W.J.: Processing of Al matrix composites reinforced with Al-Ni compounds and Al₂O₃ by reactive milling and reactive sintering, *Journal of Alloys and Compounds*, Vol. 471, pp. 448-452, 2009.
- [26] FATEMI, A., MOLAEI, R., SHARIFIMEHR, S., PHAN, N., SHAMSAEI, N.: Multiaxial fatigue behavior of wrought and additive manufactured Ti-6Al-4V including surface finish effect, *International Journal of Fatigue*, Vol. 100, pp. 347-366, 2017.
- [27] MOLAEI, R., FATEMI, A., PHAN, N.: Significance of hot isostatic pressing (HIP) on multiaxial deformation and fatigue behaviors of additive manufactured Ti-6Al-4V including build orientation and surface roughness effects, *International Journal of Fatigue*, Vol. 117, pp. 352-370, 2018.
- [28] MOLAEI, R., FATEMI, A.: Fatigue Design with Additive Manufactured Metals: Issues to Consider and Perspective for Future Research, *Procedia Engineering*, Vol. 213, pp. 5-16, 2018.

Review process

Single-blind peer review process.